The Cosmic Ray Anisotropy between 10^{14} and 10^{15} eV

The EAS-TOP COLLABORATION: M. Aglietta[1,2], B. Alessandro[2], P. Antonioli[3], F. Arneodo[4], L. Bergamasco[2,5], M. Bertaina[2,5], C. Castagnoli[1,2], A. Castellina[1,2], A. Chiavassa[2,5], G. Cini Castagnoli[2,5], B. D'Ettorre Piazzoli[6], G. Di Sciascio[6], W. Fulgione[1,2], P. Galeotti[2,5], P.L. Ghia[1,4], M. Iacovacci[6], G. Mannocchi[1,2], C. Morello[1,2], G. Navarra[2,5], O. Saavedra[2,5], G. C. Trinchero[1,2], S. Valchierotti[2,5] P. Vallania[1,2], S. Vernetto[1,2], C. Vigorito[2,5]
(1) Istituto di Fisica dello Spazio Interplanetario, CNR, Torino, Italy
(2) Istituto Nazionale di Fisica Nucleare, Torino, Italy
(3) Istituto Nazionale di Fisica Nucleare, Bologna, Italy
(4) Laboratori Nazionali del Gran Sasso, INFN, Assergi (AQ), Italy
(5) Dipartimento di Fisica Generale dell'Università, Torino, Italy
(6) Dipartimento di Scienze Fisiche dell'Università and INFN, Napoli, Italy

Abstract

The study of the anisotropy of the arrival directions is an essential and complementary tool, with respect to the energy spectrum and composition, to investigate the origin and propagation of cosmic rays primaries. In particular, the study of the evolution of the CR anisotropy over primary energy can be very powerful for the interpretation of the knee in the CR primary spectrum. By means of the EAS-TOP data (four years) we have reported an anisotropy measurement at primary energy $E_0 \approx 10^{14}$ eV [1], with amplitude $A_{sid,\delta=0^\circ} = (3.7 \pm 0.6) \cdot 10^{-4}$ and phase $\phi = (1.8 \pm 0.5)$ hr LST, at a significance level 6.5 s.d. The use of the full EAS-TOP data set and the application of different criteria of data selection allow to extend this measurement to higher energies, up to around 10^{15} eV. We report here the results of the first harmonic analysis, both in solar and sidereal time, in five energy bins.

1. The data and the analysis

The EAS-TOP Extensive Air Shower array, located at Campo Imperatore (2005 m a.s.l., lat. 42°27′N, long. 13°34′E, National Gran Sasso Laboratory), has been in operation since January 1989 up to May 2000. A detailed description of the electromagnetic detector (used for the present analysis) is given in [2]; here we summarize its main features. In its final configuration (since 1992 onward), the array consisted of 35 modules of scintillator counters, 10 m^2 each, distributed over an area $A \approx 10^5$ m^2. The trigger was provided by the fourfold coincidence

pp. 183–186

of any four neighboring modules (threshold $n_p \approx 0.3$ m.i.p./mod.), the rate being $f \approx 25$ Hz and the mean primary energy $E_0 \approx 100$ TeV.

Table 1. *Characteristics of the used classes of events.*

Class	$N_{modules}$	E_0 [TeV]	$< \beta >$ [% mbar^{-1}]	N_{events}
1	≥ 4	100	-0.69 ± 0.01	$2.1 \cdot 10^9$
2	≥ 12	300	-0.68 ± 0.01	$2.4 \cdot 10^8$
3	≥ 18	600	-0.66 ± 0.01	$8.0 \cdot 10^7$
4	≥ 24	900	-0.64 ± 0.01	$2.8 \cdot 10^7$
5	≥ 30	1200	-0.67 ± 0.02	$8.8 \cdot 10^6$

To perform the measurement as a function of primary energy, the events were classified depending on the number of triggered modules (see Table 1 for the classification, and the corresponding primary energies). All data have been corrected for atmospheric pressure variations with a regression coefficient ($\beta = 1/N(dN/dp)$) obtained for each data class separately, and for each individual run (i.e., about one week of data taking): they are shown in Tab.1, using events with $0° < \theta < 90°$. Further checks of stability based on the width, σ_{tot}, of the distributions of the counting rate for each run after the correction for pressure have been performed (runs have been disregarded mainly when affected by snow effects). The data sample is characterized by an experimental width of the counting rate distribution $\sigma^2_{tot} < 1.1 \cdot \sigma^2_{Poisson}$. The numbers of used events, for each data class, are listed in Tab.1.

2. Results and conclusions

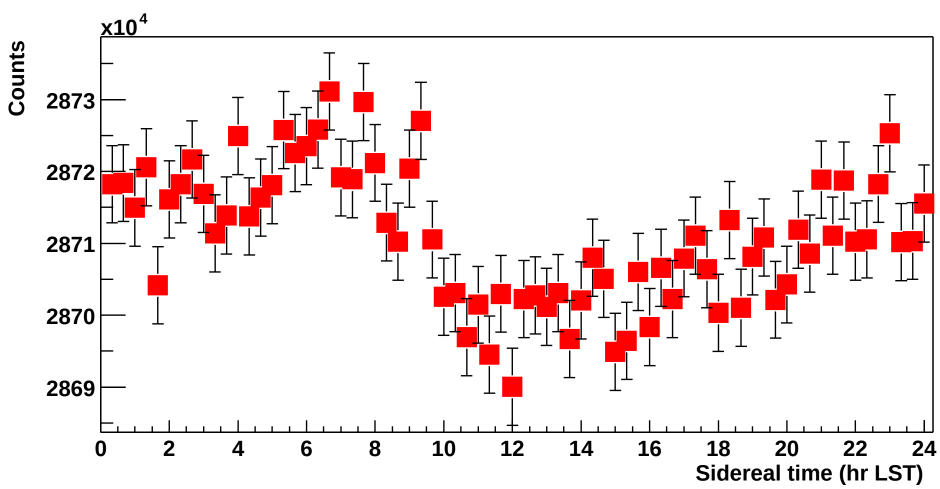

Fig. 1. *Class 1 events counting rate (in 20' bins) vs the local sidereal time.*

For the lowest energy class of data (class 1) the counting rate versus the local sidereal time in 20' time intervals is shown in Fig. 1, from which the first harmonic (significance 10.3 s.d.) over the fluctuations in the individual channels is clearly seen, the amplitude and phase being: $A = (3.4 \pm 0.3) \cdot 10^{-4}$ and $\phi = (3.3 \pm 0.4)$ hr LST. The new measurement obtained through improved statistics confirms our previous result [1]. With respect to the harmonic analysis in solar time, the results obtained with class 1 data (shown in Tab.2) are fully consistent with the ones already reported and with the expected Compton Getting effect, due to the motion of revolution of the Earth around the Sun.

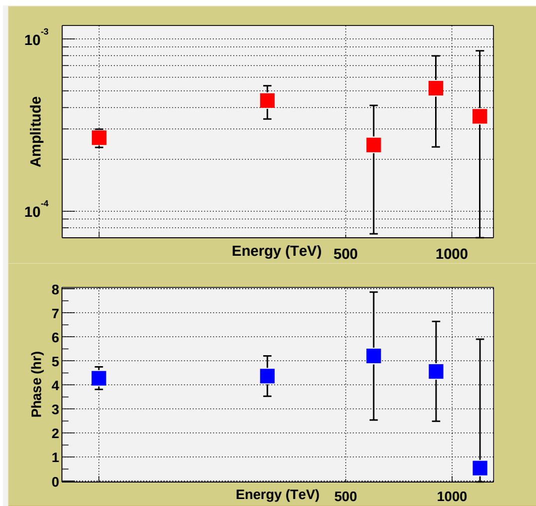

Fig. 2. *Amplitude (top) and phase (bottom) of the first harmonic in solar time vs the primary energy.*

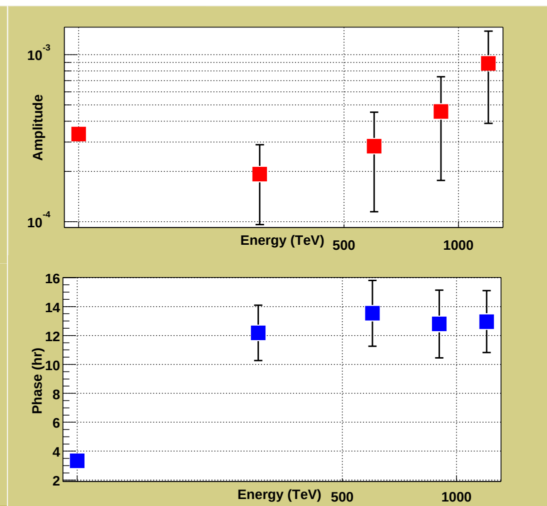

Fig. 3. *Amplitude (top) and phase (bottom) of the first harmonic in sidereal time vs the primary energy.*

The evolutions of the amplitude and phase of the first harmonic versus E_0 are shown in Figure 2 (solar time) and Figure 3 (sidereal time), and summarized in Table 2.

Table 2. *Results of the analysis of the first harmonic in solar (columns 2-4) and in sidereal time (columns 5-7), as a function of primary energy.*

E_0 [TeV]	A_{sol} (10^4)	ϕ_{sol} [hr]	A/σ	A_{sid} (10^4)	ϕ_{sid} [hr]	A/σ
100	2.7 ± 0.3	4.3 ± 0.5	8.2	3.4 ± 0.3	3.3 ± 0.4	10.3
300	4.4 ± 1.0	4.4 ± 0.8	4.6	2.0 ± 1.0	12.2 ± 1.9	2.0
600	2.4 ± 1.7	5.2 ± 2.7	1.4	2.8 ± 1.7	13.5 ± 2.3	1.7
900	5.2 ± 2.8	4.6 ± 2.1	1.8	4.6 ± 2.8	12.8 ± 2.3	1.6
1200	3.6 ± 5.0	0.5 ± 5.4	0.7	8.9 ± 5.0	13.0 ± 2.1	1.8

In solar time, a signal compatible with the Compton-Getting effect is significantly detected also in the second energy bin.

In sidereal time, at $E_0 \geq 300$ TeV, the obtained phase changes to $\phi = 12 \pm 2$ hr LST: however, the amplitudes above such energy are not significant to support such a conclusion. The derived upper limits to the amplitude of the first harmonic (corresponding to a chance probability $P = 0.0001$, following the Rayleigh probability distribution) as a function of primary energy are shown in Fig. 4 (arrows) together with the 100 TeV positive observation (square).

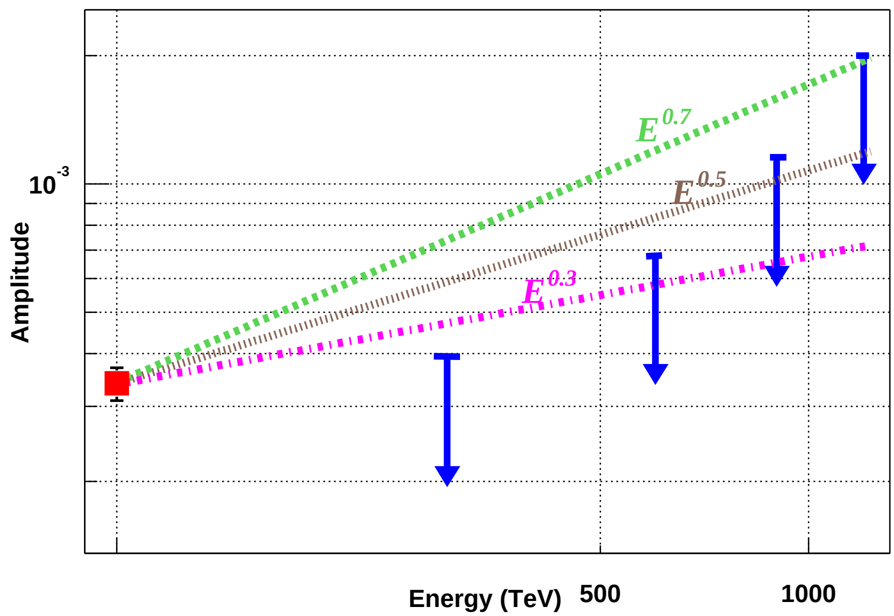

Fig. 4. *Amplitude of the first harmonic in sidereal time vs primary energy: the arrows indicate the upper limits corresponding to $P = 0.0001$. The lines correspond to possible extrapolations of the 100 TeV observation (square): the dash-dotted one represents $A \propto E^{0.3}$, the dotted one $A \propto E^{0.5}$ and the dashed one $A \propto E^{0.7}$.*

Different possible extrapolations of the amplitude observed at 100 TeV are also shown: the present data exclude increases of the 100 TeV anisotropy with laws exceeding $A \propto E^{0.3}$, which has been indicated for the energy dependence of the amplitude of the anisotropy for diffusive effects [3].

3. References

1. Aglietta M. et al. 1996, Ap. J., 470, 501
2. Aglietta M. et al. 1993, Nucl. Instr. and Meth., A336, 310
3. Dorman L.I., Gkhosh A. and Ptuskin V.S. 1984, Pis'ma Astron. Zh., 10, 827